Electron Density Analyses of Opioids: A Comparative Study

Stephan Scheins,[†] Marc Messerschmidt,[‡] Wolfgang Morgenroth,[§] Carsten Paulmann,[||] and Peter Luger*,[†]

Institute for Chemistry and Biochemistry/Crystallography, Free University of Berlin, Fabeckstr. 36a, 14195 Berlin, Germany, DESY/HASYLAB, Notkestr 85, 22603 Hamburg, Germany, Institute for Inorganic Chemistry, Georg August Universität, Tammannstr. 4, 37077 Göttingen, Germany, Department of Chemistry, Aarhus University, Langelandsgade 140, 8000 Aarhus C, Denmark, c/o DESY/HASYLAB, Notkestr 85, 22603 Hamburg, Germany, and Mineralogisch-Petrologisches Insitut, Universität Hamburg, Grindelallee 48, 20146 Hamburg, Germany

Received: February 2, 2007; In Final Form: April 13, 2007

The electron densities of five morphine related molecules (codeine, diprenorphine, naltrexone in the neutral and protonated states, and dextromethorphan) were determined from high-resolution X-ray diffraction experiments (Mo Kα and synchrotron primary radiation) at low temperature and CCD area detection techniques. Bond topological analyses were applied, and a partitioning of the molecules into atomic regions making use of Bader's zero flux surfaces yielded atomic volumes and charges. The obtained atom and bonding properties were compared to the results of a previous experimental study of morphine and to theoretical calculations. Experimental and theoretical properties for all chemically equivalent bonds agree within an uncertainty range as is otherwise seen for different theoretical calculations. Hence, the transferability of chemically equivalent submolecular properties, being a key issue of the atoms in molecules (AIM) theory, has been verified experimentally in this class of chemically related molecules. On the other hand, topological differences could clearly be verified in regions with different chemical environments. Electron density differences between the two forms of naltrexone were examined and made visible in an extendend region around the nitrogen atom which is once in a neutral state and once in a positively charged state.

1. Introduction

Due to recent developments in computer and detector technology, systematic and comparative experimental charge density studies of entire classes of compounds can be carried out in an acceptable amount of time even if the molecules are getting larger. This has been done so far for amino acids[1] and oligo peptides.[2−4] Here, the results of a further comparative charge density study of morphine and morphine related compounds are presented.

In addition to their biological activity, these opioids are also of interest because of their variety of chemical features. They consist of an oligocyclic strained cage structure containing aromatic rings, heterocyclic rings, five- and six-membered rings in different conformations (three-membered rings in some cases), aliphatic regions, and phenolic as well as methoxy oxygen atoms. We examined the charge densities of morphine hydrate (**1**)[5] and four related substances obtained from high-resolution X-ray experiments at low temperature and CCD area detection. The results were interpreted according to Bader's theory of atoms in molecules (AIM).[6] The transferability, a key concept of the AIM theory, was intended to be experimentally confirmed for the unusual bonding situation in the strained ring systems. Morphine, the principal active agent in opium, is a powerful opioid analgesic drug. Codeine (**2**) is predominantly used for its antitussive and antidiarrheal properties. The structure is similar to that of morphine, except that a methyl group replaces the hydrogen atom at the atom O1 (for atom numbering see Figure 1). Diprenorphine (**3**) is a potent nonselective opioid antagonist. Naltrexone (**4a** = neutral, **4b** = protonated formate salt) is an opioid receptor antagonist used primarily in the treatment of alcohol and opioid dependencies. The tertiary amine methyl substituent is replaced by methylcyclopropane. A hydroxy group is added at C14 and a carbonyl group is found on C6. Dextromethorphan (**5**) is also an antitussive drug, but the perceived advantage of dextromethorphan in comparison to codeine is the lack of physical addiction. Compared to morphine, the molecule has only one oxygen atom O1 and a single bond C7−C8. Except for one case, the compounds considered here are the free bases. In the case of naltrexone (**4a** and **4b**), we succeeded in crystallizing, in addition to the free base, the form where the nitrogen atom is protonated. In this form, it is present under physiological conditions.

While the sequences, but not the exact three-dimensional structures, of the related opioid receptors are known, the site and type of substrate-receptor recognition and interaction are not known.[7−9] Therefore, it would be highly speculative to draw conclusions from the charge densities of the considered opioids to their different activities in the human body. Thus, the focus of this study was directed to the transferability of submolecular properties also in this class of chemically related compounds. This question is of crucial and actual importance in the development of database approaches in charge density work[10−12] in progress in different groups where transferability is an essential provision for their application.

* To whom correspondence should be addressed.
[†] Free University of Berlin.
[‡] DESY/HASYLAB.
[§] Georg August Universität.
[||] Universität Hamburg.

10.1021/jp0709252 CCC: $37.00
Published on Web 05/26/2007

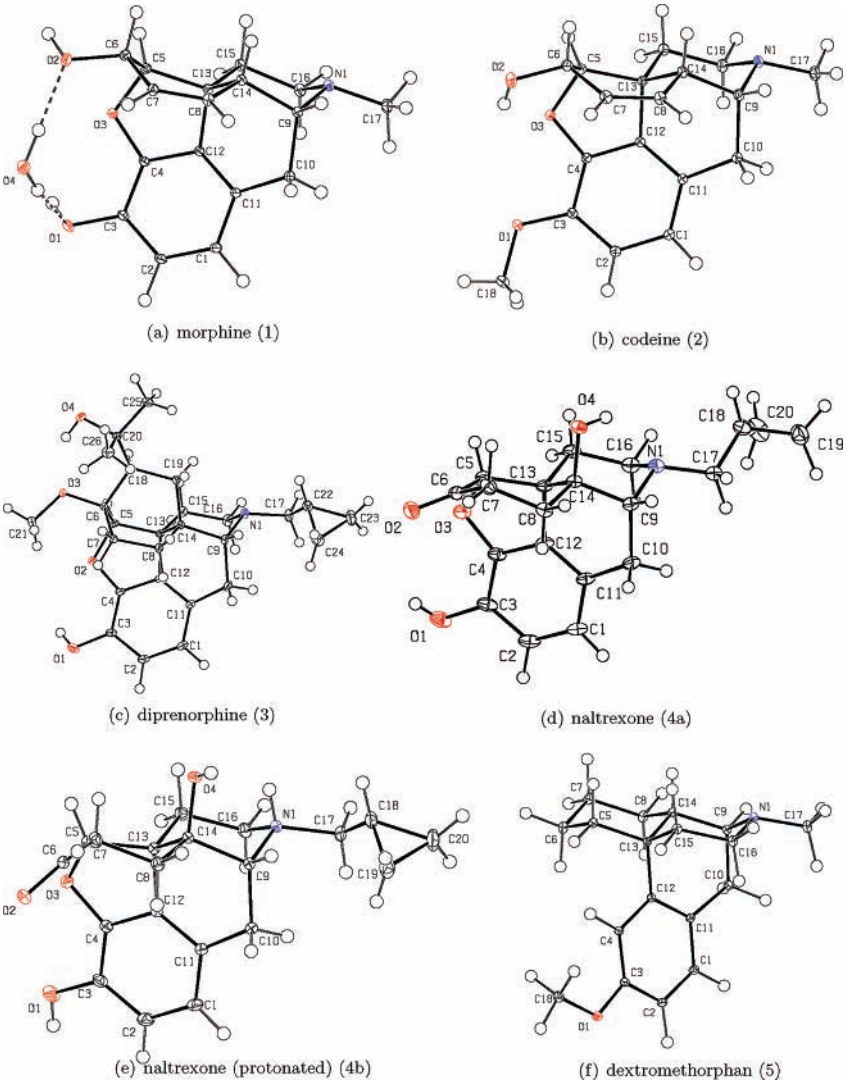

Figure 1. ORTEP representations[24] of the compounds (50% probability) with atom numbering schemes as derived from X-ray experiments: morphine (**1**), top left; codeine (**2**), top right; diprenorphine (**3**), second row left; naltrexone (**4a**), second row right; protonated naltrexone (**4b**), bottom left; and dextromethorphan (**5**), bottom right.

TABLE 1: Crystallographic Data and Figures of Merit

cpd	codeine	diprenorphine	naltrexone	naltrexone formate	dextromethorphane
exp station	home	D3	D3	F1	home
formula	$C_{18}H_{21}NO_3$	$C_{26}H_{35}NO_4$	$C_{20}H_{23}NO_4 \cdot H_2O$	$C_{20}H_{24}NO_4 \cdot 4H_2O \cdot CHO_2$	$C_{18}H_{25}NO$
cryst sys	orthorhombic	orthorhombic	monoclinic	orthorhombic	orthorhombic
space group	$P2_12_12_1$ (No. 19)	$P2_12_12_1$ (No. 19)	$P2_1$ (No. 14)	$P2_12_12_1$ (No. 19)	$P2_12_12_1$ (No. 19)
Z	4	4	4	4	4
a [Å]	7.335(13)	11.991(2)	14.494(17)	7.993(2)	7.0476 (4)
b [Å]	13.647(9)	12.099(9)	7.666(9)	15.339(9)	13.934(7)
c [Å]	14.735(13)	15.707(4)	16.672(13)	18.791(4)	14.825(8)
β[°]	90.0	90.0	105.66(1)	90.0	90.0
V [Å^3]	1474.97(5)	2278.84(8)	1783.69(3)	2303.90(8)	1455.76(14)
D_x [g cm^{-3}]	1.348	1.240	1.339	1.323	1.238
cryst size	0.6 × 0.4 × 0.3	0.4 × 0.4 × 0.3	0.4 × 0.12 × 0.12	0.4 × 0.1 × 0.1	0.4 × 0.4 × 0.4
λ [Å]	0.71073	0.5500	0.5600	0.5600	0.71073
μ [mm^{-1}]	0.09	0.05	0.06	0.06	0.08
temp [K]	20	100	100	100	20
$(\sin\theta/\lambda)_{max}$ [Å^{-1}]	1.10	1.21	1.22	1.11	1.15
reflns collected	68674	370413	170872	292875	84785
unique reflns	8217	17998	26780	12430	9773
R_{int}	0.0361	0.0450	0.0350	0.0721	0.0392
reflns incl in mult refs	7525	11408	22805	8382	8717
$R(F)$	0.0204	0.0256	0.0195	0.0294	0.0182
$R_w(F)$	0.0180	0.0120	0.0186	0.0330	0.0195
GOF	0.95	2.45	1.81	0.70	0.80

As will be detailed below for the six compounds of this study, a good agreement concerning the transferability of atomic and bond topological properties of chemically related parts of the molecules was found. Additionally, changes of the chemical environment could be detected clearly and visualized. The comparison of the neutral and protonated naltrexone allowed

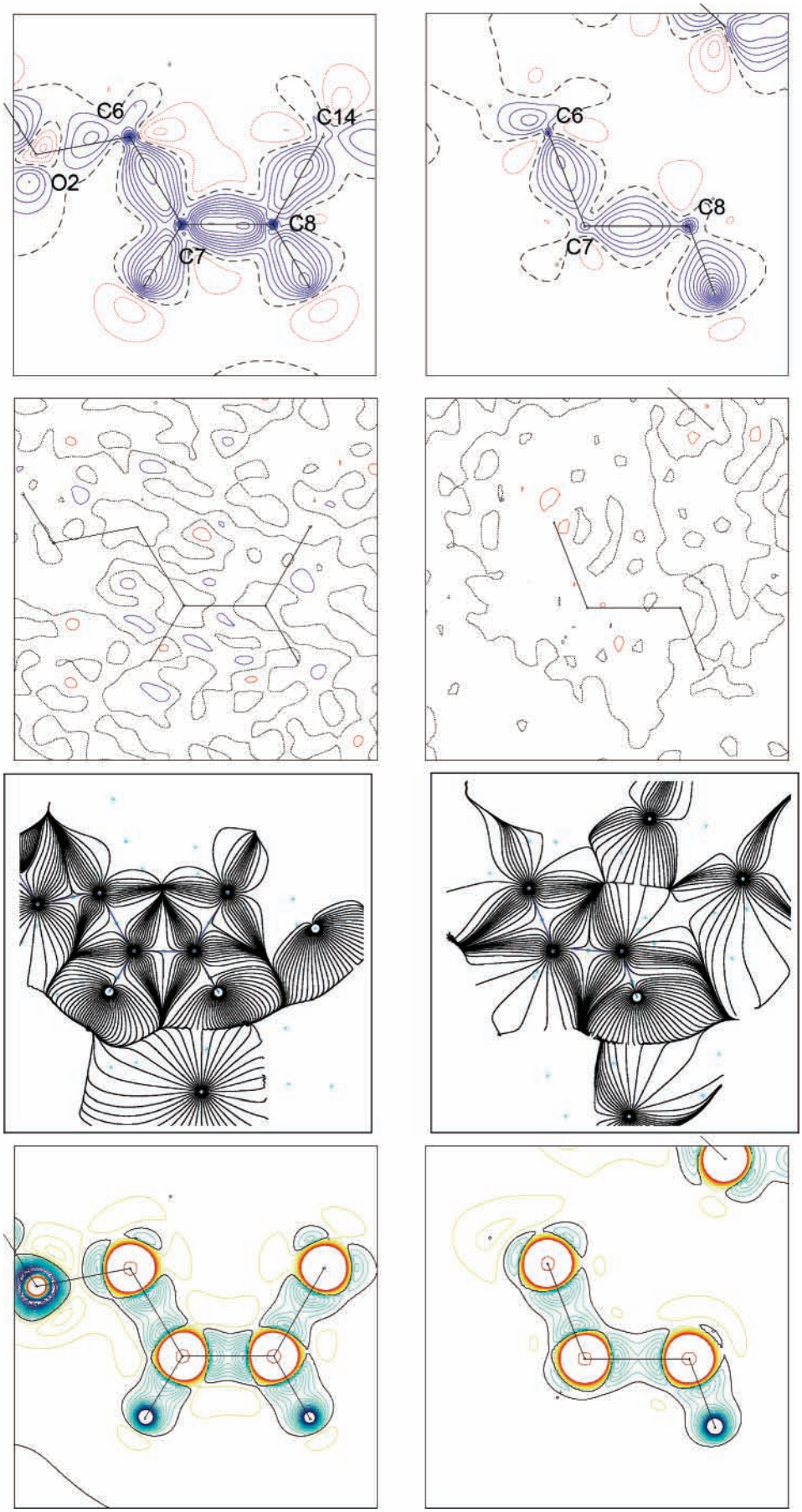

Figure 2. C7−C8 bond of morphine (left side) and naltrexone (right side) in terms of static deformation density maps (top row, contour interval = 0.1 e Å^{-3}, blue/red = positive/negative values); (second row) corresponding residual densities; (third row) gradient vector fields of the bond C7−C8; and (bottom row) Laplace distribution (contour interval = 5 e Å^{-5}, blue/red = negative/positive values) of the same bond.

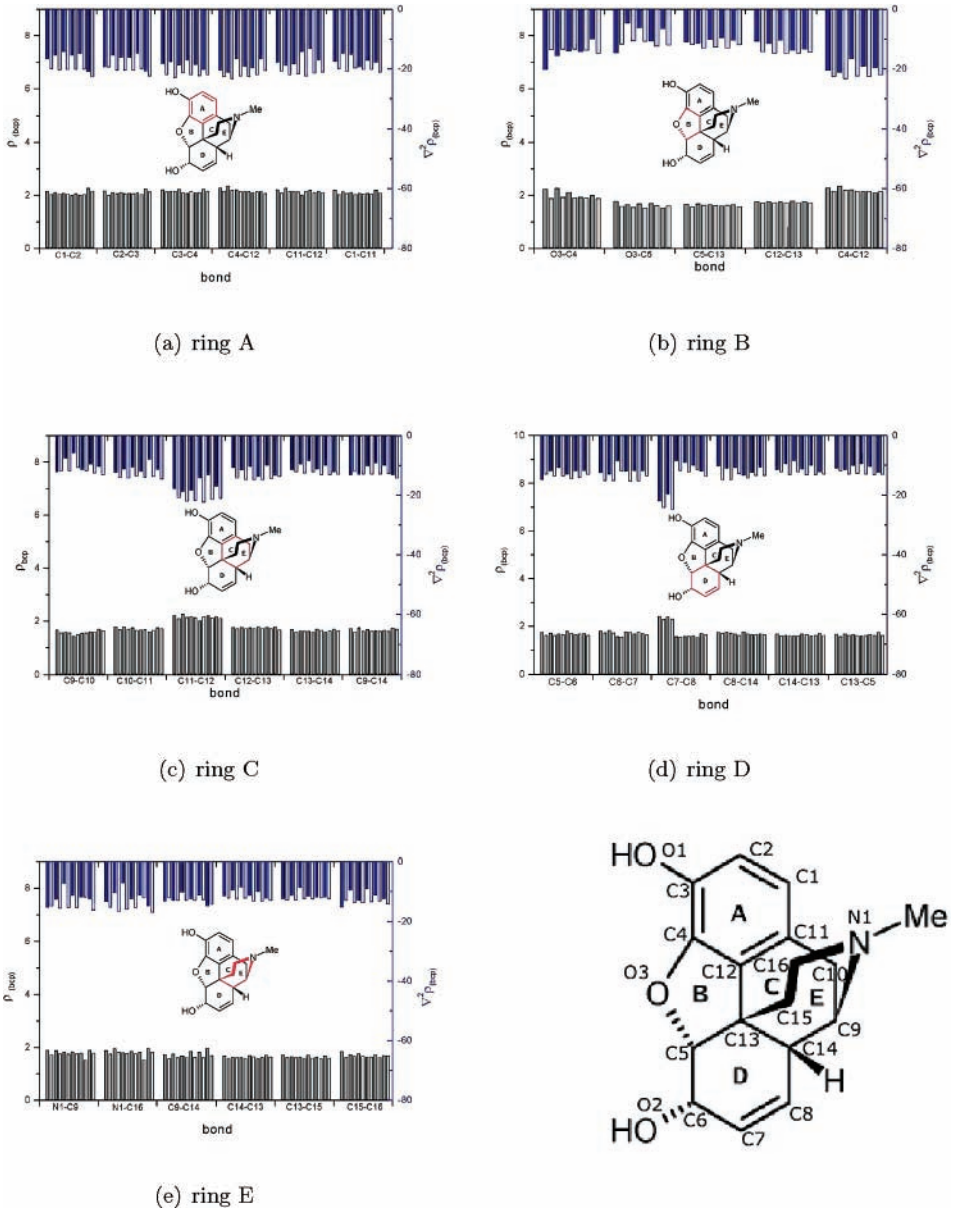

Figure 3. Electron density and Laplacian at the bcp. Each diagram represents one ring of the oligocyclic opiate skeletal structure. The lower bars show ρ at the bcps (dark gray for the experimental values and light gray for the theoretical ones); the upper bars display the Laplacians at the bcp (dark blue for the experimental values and light blue for the theoretical ones). The order of the bars of each bond is morphine (**1**), codeine (**2**), diprenorphine (**3**), naltrexone (**4a**), naltrexone formiate (**4b**), and dextrometorphan (**5**). The labeling of the ring systems and atomic numbering is given by the picture (right) in the third row.

examination of the changes of the electron density, especially in the region around the nitrogen, which is once in a neutral state and once in a formal positive charge state.

2. X-ray Diffraction Experiments

Crystals were grown by slow evaporation of ethanol/water solutions. High-resolution X-ray diffraction data were collected at three experimental setups:

(i) with Mo Kα radiation (graphite monochromator) at 20 K on our in-house four-circle Huber diffractometer (type 512) equipped with a double stage closed cycle He cryostat (Displex, Air Products), a new 0.1 mm Kapton-film vacuum chamber around the cold head,[13] and a Bruker-APEX area detector;

(ii) with synchrotron radiation at wavelengths at ~0.55 Å at the beamlines F1 and D3 of the storage ring DORIS III at the HASYLAB/DESY, Hamburg, Germany. Beamline F1 is equipped with a κ-axis diffractometer, while at D3 a Huber four-circle diffractometer is in use. For the synchrotron measurements, the temperature at the crystal site was maintained at 100 K with an Oxford Cryosystem N_2 gas stream cooling device. The diffraction intensities were collected with a MarCCD-165 area detector.

The frames were integrated and scaled with the SAINT and SORTAV programs[14] for the in-house X-ray measurements and with XDS[15] and SORTAV for the synchrotron data. Further details on the crystal data and the experimental conditions are given in Table 1.

3. Density Models and Refinement Strategy

The conventional (spherical) X-ray structures of **2** and **5** were known from the literature,[16,17] while those of **3**, **4a**, and **4b** were unknown. Nevertheless, all structures were determined or redetermined and spherically refined[18] to enter the low-temperature spherical models as starting atomic parameters into the further aspherical atom treatment. The generalized scattering

TABLE 2: Ring Critical Points of the Oligocyclic Opiate Skeletal Structures[a]

	ring A		ring B		ring C		ring D		ring E	
cpd	ρ	$\nabla^2\rho$	ρ	$\nabla^2\rho$	ρ	$\nabla^2\rho$	ρ	$\nabla^2\rho$	ρ	$\nabla^2\rho$
morphine	0.20(1)	3.0(1)	0.37(1)	5.5(1)	0.17(1)	2.5(1)	0.16(1)	2.3(1)	0.15(1)	2.4(1)
codeine	0.19(3)	3.0(1)	0.32(2)	5.8(1)	0.15(2)	2.5(1)	0.13(2)	2.5(1)	0.15(3)	2.4(1)
diprenorphine	0.17(2)	3.0(1)	0.30(2)	5.4(1)	0.15(1)	2.4(1)	0.17(2)	2.4(1)	0.17(2)	2.4(1)
naltrexone	0.19(1)	2.8(1)	0.35(2)	5.7(1)	0.17(2)	2.3(1)	0.16(3)	2.3(1)	0.16(2)	2.3(1)
naltrexone formate	0.16(2)	2.8(1)	0.37(2)	6.0(1)	0.17(3)	2.3(1)	0.14(2)	2.3(1)	0.15(2)	2.3(1)
dextromethorphan	0.16(2)	2.9(1)			0.13(3)	2.3(1)	0.14(2)	2.4(1)	0.14(2)	2.5(1)

[a] All values are given in e Å^{-3} (ρ) and e Å^{-5} ($\nabla^2\rho$).

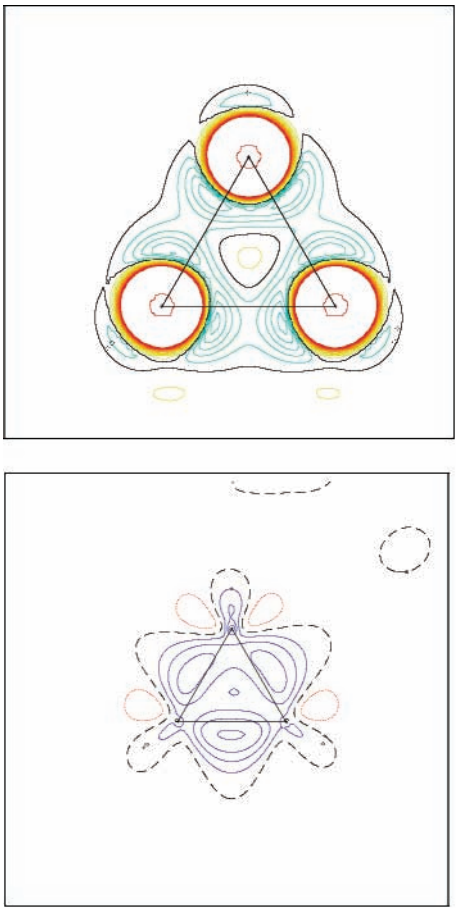

Figure 4. Laplace distribution (top, contour interval = 5 e Å^{-5}, blue/red = negative/positive values) and static deformation density (bottom, contour interval = 0.1 eÅ^{-3}, blue/red = positive/negative values) of the three-membered ring of naltrexone.

factor model based on the Hansen−Coppens formalism[19] was applied in the multipole refinements which were carried out with the full-matrix LSQ program (XDLSM) of the XD program package.[20] Hydrogen atom positions were kept fixed to be at standard neutron distances to their parent atoms.[21] The hexadecapolar level of the multipolar expansion was used for carbon, nitrogen, and oxygen atoms, while bond directed dipoles were used for hydrogen atoms. Local site symmetry was used when chemically reasonable. A local mirror symmetry was applied to the carbon atoms in the phenyl ring, while C_{3v} symmetry was imposed for the methyl groups. No symmetry restriction was imposed on the oxygen atom of the hydroxyl group, as it is involved in hydrogen bonding. Only symmetry independent reflections, which met the criterion $F_{obs}(H) > 2.5\sigma F_{obs}(H)$, were included in the refinements. Agreement factors for the five data sets after convergence of the multipole refinements are listed in Table 1.

4. Theoretical Calculations

The GAUSSIAN98 program package[22] was used for *ab initio* calculations at the density functional (B3LYP) level of theory. For each molecule, the basis set 6-311++G(3df,3pd) was used for a single point calculation at the experimental geometry. The wave functions obtained were evaluated with the program package AIMPAC.[23]

5. Results and Discussion

The molecular structures of the six compounds as derived from X-ray experiments are displayed as ORTEP[24] representations in Figure 1.

To illustrate a few qualitative features, the C7−C8 bonds of morphine and naltrexone are displayed exemplarily by their static deformation densities, residual maps, and, making use of the first and second partial derivatives of $\rho(\mathbf{r})$, the gradient vector field $\nabla\rho(\mathbf{r})$ and the Laplacian $\nabla^2\rho(\mathbf{r})$ in Figure 2. While in the case of the sp^2 carbon atoms of morphine the two hydrogens are in the plane C6−C7−C8, only one hydrogen is in this plane in the case of the sp^3 carbon atoms as it is shown in the gradient vector field. The C═C double bond of morphine shows a higher deformation density peak than the C−C single bond of naltrexone. The Laplacian distributions in Figure 2 (fourth row) support the qualitative findings shown by the static deformation maps. No significant electron density was found in the residual density maps (second row) that includes all reflections (no resolution cut off), indicating an adequate description of the experimental data by the multipole model.

5.1. Bond Topological Properties. To obtain a quantitative description of the electronic structure of the molecules, a full topological analysis was performed with the XDPROP part of the XD program package.[20] Bond critical points (bcp, defined by the property that at a bcp the gradient $\nabla\rho(\mathbf{r})$ vanishes) were found on all covalent bonds. Figure 3 shows the values of $\rho(\mathbf{r})$ and $\nabla^2\rho(\mathbf{r})$ at the bcps for the covalent bonds, whereas each diagram represents one ring of the oligocyclic opiate skeletal structure.

The lower bars show the electron density values at the bond critical points (dark gray for the experimental values and light gray for the theoretical ones), while the upper bars display the Laplacians at the bcp (dark blue for the experimental values and light blue for the theoretical ones). The sequence of the bars of each bond is morphine (**1**), codeine (**2**), diprenorphine (**3**), naltrexone (**4a**), naltrexone formate (**4b**), and dextromethorphan (**5**). Since the bridging oxygen atom is missing in the case of dextromethorphan (**5**), only five values for each bond are given in the diagram of ring B. For the case of naltrexone, the average values of the two molecules in the asymmetric unit are given. In general, it was found that the statistical differences between theory and experiment are small for $\rho(\mathbf{r}_{bcp})$ (0.12 eÅ^{-3}) and moderate for $\nabla^2\rho(\mathbf{r}_{bcp})$ (2.87 e Å^{-5}). For the nonpolar C−C bonds, the deviation is fair, while for the polar bonds the difference is significantly larger.

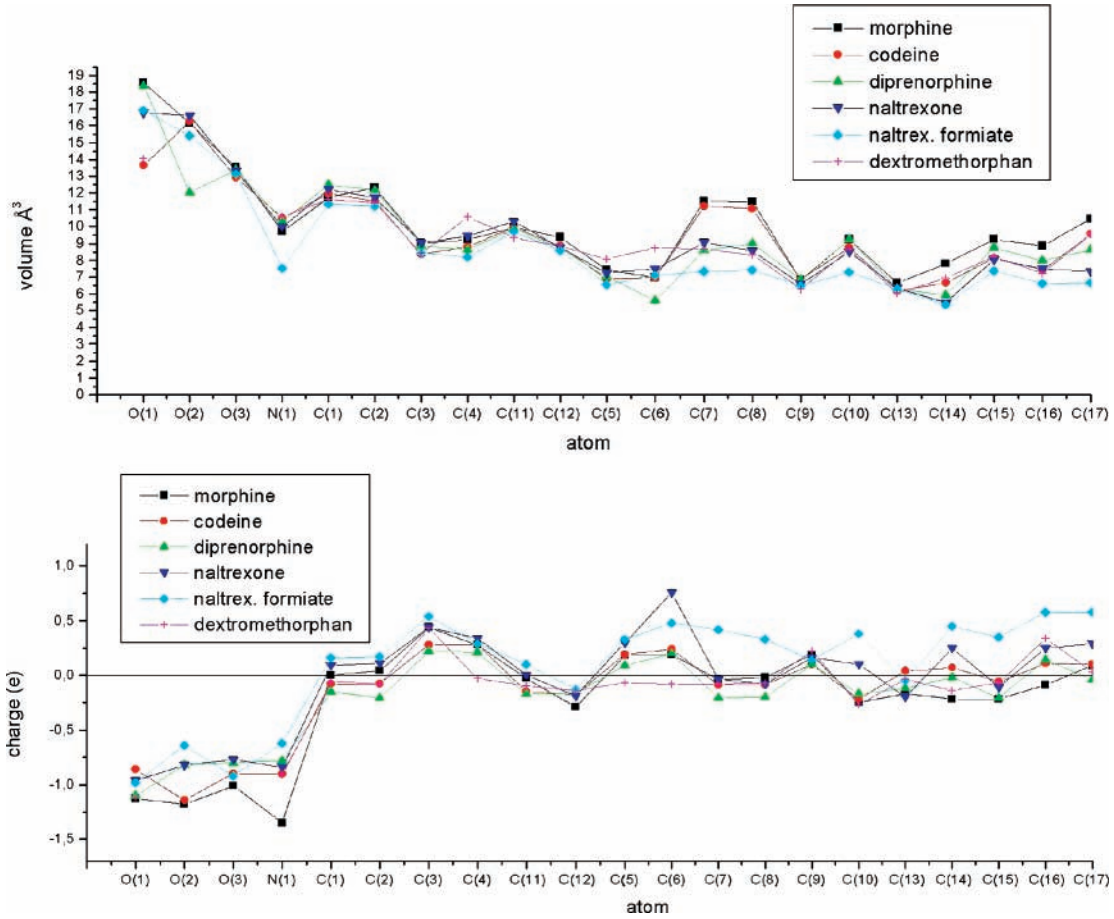

Figure 5. Atomic volumes (top) and charges (bottom) of the oligocyclic skeletal structure.

With a reliability factor defined as

$$R_\rho = \sum|\rho_{exp} - \rho_{th}|/\sum\rho_{exp} \quad (1)$$

the agreement between the experiment and the theory can be analyzed. This results in a R_ρ value of 0.046 for the electron density at the bond critical points. This R_ρ value is nearly identical to the corresponding value for strychnine (R_ρ = 0.047).[30] The 93 C−C single bonds give experimentally an average $\rho(\mathbf{r}_{bcp})$ value of 1.68(7) e Å^{-3} and $\nabla^2\rho(\mathbf{r}_{bcp})$ value of −11.7(25) e Å^{-5}. In the diagram of ring D, the difference with respect to the nature of the C7−C8 bond between the molecules is visible. While morphine and codeine contain a double bond here ($\rho(\mathbf{r}_{bcp})$ = 2.431 and 2.401 e Å^{-3}, respectively, and $\nabla^2\rho(\mathbf{r}_{bcp})$ = −22.2 and −19.9 e Å^{-5}, respectively), the other molecules have a normal single bond.

The experimentally received mean values for the aromatic bonds ($\rho(\mathbf{r}_{bcp})$ = 2.15(8) eÅ^{-3} and $\nabla^2\rho(\mathbf{r}_{bcp})$ = −17.6(16) e Å^{-5}) lie in between the single and the double bonds, as expected. For the C−N bonds, a difference of 15% between the free bases and the protonated nitrogen atom of **4b** is observed. The C−N bonds of the unprotonated molecules give $\rho(\mathbf{r}_{bcp})$ = 1.87(6) e Å^{-3} and $\nabla^2\rho(\mathbf{r}_{bcp})$ = −12.5(23) e Å^{-5}, while for **4b** we found $\rho(\mathbf{r}_{bcp})$ = 1.63(4) e Å^{-3} and $\nabla^2\rho(\mathbf{r}_{bcp})$ = −6.7(13) e Å^{-5}. For the polar C−O bonds C4−O3 and C5−O3 of the ring system B (upper row, middle), the mean values are $\rho(\mathbf{r}_{bcp})$ = 2.11 (14) and 1.67(9) e Å^{-3} or rather $\nabla^2\rho(\mathbf{r}_{bcp})$ = −15.0(37) and −8.7(41) e Å^{-5}.

Table 2 shows the characteristic data for the ring critical points of the oligocyclic opiate skeletal structure. The congruence between the different experiments shows that the electron density is also adequately described far away from the nuclei.

Three compounds (**3**, **4a**, and **4b**) contain, in addition to the morphine-like skeletal structure, a cyclopropane ring. Exemplarily, the Laplacian and the static deformation density of the three-membered ring of naltrexone (**4a**) is shown in Figure 4. The strain in the three-membered ring is clearly visible by the minima of the saddle shape regions of the Laplacian and the maxima of the deformation density outside the direct internuclear vectors indicating the bent character of the bonds in this region. The displacements of the bcp of the C−C bonds from the internuclear lines are 0.021 Å, which are in good agreement with the results of a barbaralane derivative (0.023 Å).[25]

5.2. Atomic Properties. As mentioned before, a molecule can be divided into submolecular fragments according to Bader's AIM theory. For the evaluation of atomic volumes and charges, the program TOPXD[26] was used. Figure 5 shows the results of the integration of the non-H skeletal structure. The upper diagram represents the experimental atomic volumes V_{001} (defined by the cutoff at ρ = 0.001 au; all atomic properties are given in the supplement), while the lower one contains the atomic charges. A broad distribution is observed for the volume of O1, whereas codeine and dextromethorphan show the smallest value because in this case a methyl group is connected to the oxygen atom, while for the other molecules the oxygen atom is part of a hydroxyl group. The same trend is seen for O2, where diprenorphine with a CH_3 group has a smaller volume compared to the other compounds. Thereby, the volume of a hydroxyl oxygen atom and a carbonyl oxygen (**4a** and **4b**) is nearly the same. The volume of O3 in the five-membered heterocyclic ring is, if present, almost constant. In the case of N1, only the protonated nitrogen atom of **4b** is smaller and hence is different

TABLE 3: Hydrogen Bonds and Weak Interactions[a]

	D−H···A	symm op	$\rho(\mathbf{r}_{bcp})$	$\nabla^2\rho(\mathbf{r}_{bcp})$	H···A	D···A	D−H	D−H−A	E_{HB}
morphine	O1−H11···N1	$2-x, -1/2+y, 1/2-z$	0.27(4)	6.0(1)	1.6743	2.6352(6)	0.9700	170.12	61.01
	O2−H21···O4	$1/2+x, 3/2-y$, 1 -z	0.16(1)	5.0(1)	1.7364	2.7022(7)	0.9695	173.76	48.79
	O4−H41···O2		0.20(4)	0.3(2)	1.8267	2.6723(7)	0.9685	178.32	35.25
	O4−H42···O1		0.15(1)	0.9(1)	2.0064	2.9668(6)	0.9697	170.36	18.46
	C8−H8···O1	$1-x, -1/2+y, 1/2-z$	0.06(1)	1.2(1)	2.2690	3.1739(7)	1.0799	140.09	7.17
	C9−H9···O3	$2-x, -1/2+y, 1/2-z$	0.05(1)	0.9(1)	2.4791	3.3206(6)	1.0805	133.87	3.37
codeine	C6−H6···O2	$-1/2+x, 1/2-y, 1-z$	0.03(1)	0.9(1)	2.3423	3.2434(6)	1.0800	139.85	5.51
	C10−H101···O3	$3/2-x, -y, -1/2+z$	0.07(1)	1.2(1)	2.4167	3.4364(6)	1.0799	156.94	4.21
diprenorphine	O1−H11···O4	$-1/2+x, -1/2-y, z$	0.11(2)	4.2(1)	1.7574	2.6929(7)	0.9700	161.47	45.24
	O4−H41···O2		0.11(1)	3.4(1)	1.8324	2.6723(7)	0.9700	142.92	34.53
	C21−H121···O3		0.06(1)	1.1(1)	2.3678	3.1615(7)	1.0800	128.91	5.03
naltrexone	O1W−H1W···O2A	$1-x, -1/2+y, -z$	0.04(1)	1.5(1)	2.1223	3.0518(7)	0.9564	163.61	12.16
	O1W−H1W···O3A	$1-x, -1/2+y, -z$	0.06(1)	1.0(1)	2.4165	2.9948(5)	0.9564	118.63	4.22
	O1W−H2W···O4A	$-1+x, -1+y, z$	0.10(3)	3.1(1)	1.9412	2.8854(6)	0.9571	168.46	23.34
	O2W−H3W···O4		0.10(2)	2.6(1)	1.9989	2.9454(7)	0.9559	170.21	18.96
	O4A−H4A···O2W	$1+x, 1+y, z$	0.04(1)	0.7(1)	2.5924	3.1126(6)	0.9684	113.84	2.24
	O2W−H4W···O3	$1-x, -1/2+y, 1-z$	0.04(1)	0.8(1)	2.5004	3.0831(6)	0.9563	119.28	3.12
	O1−H11···O2W	$1-x, 1/2+y, 1-z$	0.19(3)	3.7(1)	1.8403	2.8028(8)	0.9710	170.67	33.56
	O1A−H11A···O1W	$1-x, 1/2+y, -z$	0.21(3)	3.6(1)	1.8026	2.7562(7)	0.9725	165.95	38.44
	O4−H41···O1W		0.07(1)	1.3(1)	2.2401	2.9624(6)	0.9692	130.47	7.96
	C20A−H20B···O1	$2-x, -1/2+y, -z$	0.04(1)	0.7(1)	2.5219	3.3964(6)	1.0943	136.11	2.89
	C8−H82···O2	$1-x, 1/2+y, 1-z$	0.03(1)	0.7(1)	2.4636	3.4883(7)	1.0936	155.48	3.56
	C17−H172···O2A	$1-x, -1/2+y, -z$	0.05(1)	0.8(1)	2.4840	3.2496(5)	1.0939	125.98	3.31
naltrexone+H	O1−H11···O7	$1-x, 1/2+y, 3/2-z$	0.23(1)	3.2(1)	1.8487	2.715(3)	0.9703	169.43	45.19
	O4−H41···O5	$-1+x, y, z$	0.17(1)	2.2(1)	1.9981	2.8104(18)	0.9693	166.53	31.01
	N1−H111···O2	$-1+x, y, z$	0.13(1)	1.8(1)	2.1967	2.8612(16)	0.9289	127.88	9.32
	N1−H111···O4		0.17(1)	2.5(1)	2.1236	2.6726(8)	0.9289	116.77	12.14
	O11−H121···O7	$1/2+x, 1/2-y, 1-z$	0.12(1)	1.7(1)	2.2021	2.968(3)	0.8696	147.34	9.13
	O11−H122···O8	$1+x, y, z$	0.24(1)	3.1(1)	1.9092	2.838(2)	0.9310	171.41	25.96
	O7−H772···O5	$-1+x, y, z$	0.25(1)	3.2(1)	1.9405	2.771(2)	0.9701	177.34	38.86
	O8−H881···O9	$-x, -1/2+y, 3/2-z$	0.24(1)	3.3(1)	1.8849	2.753(2)	0.9698	168.30	38.68
	O8−H882···O6	$-1/2+x, 1/2-y, 1-z$	0.19(1)	2.8(1)	2.0084	2.7790(3)	0.9700	177.69	38.07
	O9−H991···O5	$3/2-x, 1-y, 1/2+z$	0.16(1)	2.2(1)	2.0497	2.876(2)	0.9702	165.97	24.22
	O9−H992···O3	$1-x, -1/2+y, 3/2-z$	0.11(1)	1.6(1)	2.1813	2.914(18)	0.9697	159.65	19.52
	C7−H71···O6		0.06(1)	0.9(1)	2.5431	3.4627(2)	1.0799	177.38	4.76
	C8−H82···O5	$-1+x, y, z$	0.04(1)	0.7(1)	2.5965	3.3970(19)	1.0803	133.43	2.43
	C17−H171···O8	$-x, 1/2+y, 3/2-z$	0.07(1)	1.0(1)	2.4520	3.3912(19)	1.0801	169.86	5.89
dextromethorphan	C2−H2···N1	$1-x, 1/2+y, 3/2-z$	0.04(1)	0.6(1)	2.6015	3.4752(4)	1.0801	137.50	2.17
	C18−H18···O1	$-1/2+x, 3/2-y, 2-z$	0.04(1)	0.9(1)	2.4270	3.4176(5)	1.0806	151.78	4.06

[a] Units: distances (Å), angles (°), ρ (e Å^{-3}), $\nabla^2\rho$ (e Å^{-5}), and E_{HB} (kJ mol^{-1}).

compared to the rest due to an additional substituent. For all compounds, the volumes of the aromatic carbons of ring A are comparable except for C4 of dextromethorphan (**5**), which is not connected to an oxygen atom like the rest. Within the six atoms of the aromatic ring A, C1 and C2, which always carry a hydrogen atom, have therefore a higher volume than the other four atoms, which have three non-hydrogen atoms as their nearest neighbors. A similar observation is made for C5 and C6 of molecule **5**. In these cases, the oxygen atoms are missing. At C7 and C8, the molecules containing a C═C double bond (morphine (**1**) and codeine (**2**)) have a higher volume than the molecules with a C−C single bond. The carbon atoms around the nitrogen atom show a wider spread, since C17, for example, is part of a methyl group (morphine (**1**), codeine (**2**), and dextrometorphan (**5**)) or a methylene group (diprenorphine (**3**), naltrexone (**4a**), and naltrexone formate (**4b**)).

The experimental charges of the oxygen and nitrogen atoms are all strongly negative. The amount of negative charge depends obviously on the strength of the interatomic interaction, as, for example, for morphine where the atoms O1, O2, and N1, being involved in strong hydrogen bonds, yield a large negative charge. Strong differences with respect to the positive charges are seen for C6, which is connected to a carbonyl oxygen in the case of naltrexone (**4a** and **4b**), whereas in the other compounds this carbon atom is connected to a hydroxy (**1** and **2**), methoxy (diprenorphine (**3**)) or methylene group (dextromethorphan (**5**)).

While the atomic volumes of the carbon atoms around the protonated nitrogen atom of **4b** are systematically smaller

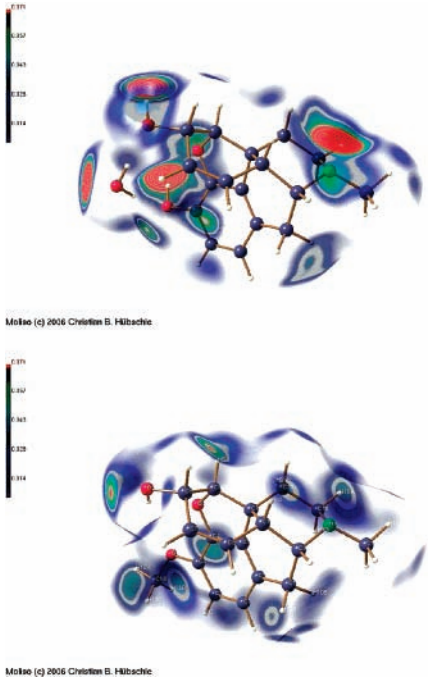

Figure 6. Three-dimensional representations of the Hirshfeld surface for the morphine and codeine molecules calculated from the experimental charge densities (drawing generated with MOLISO[31]). The crystal electron density (e Å^{-3}) is mapped by a color code onto the surface; see color bar.

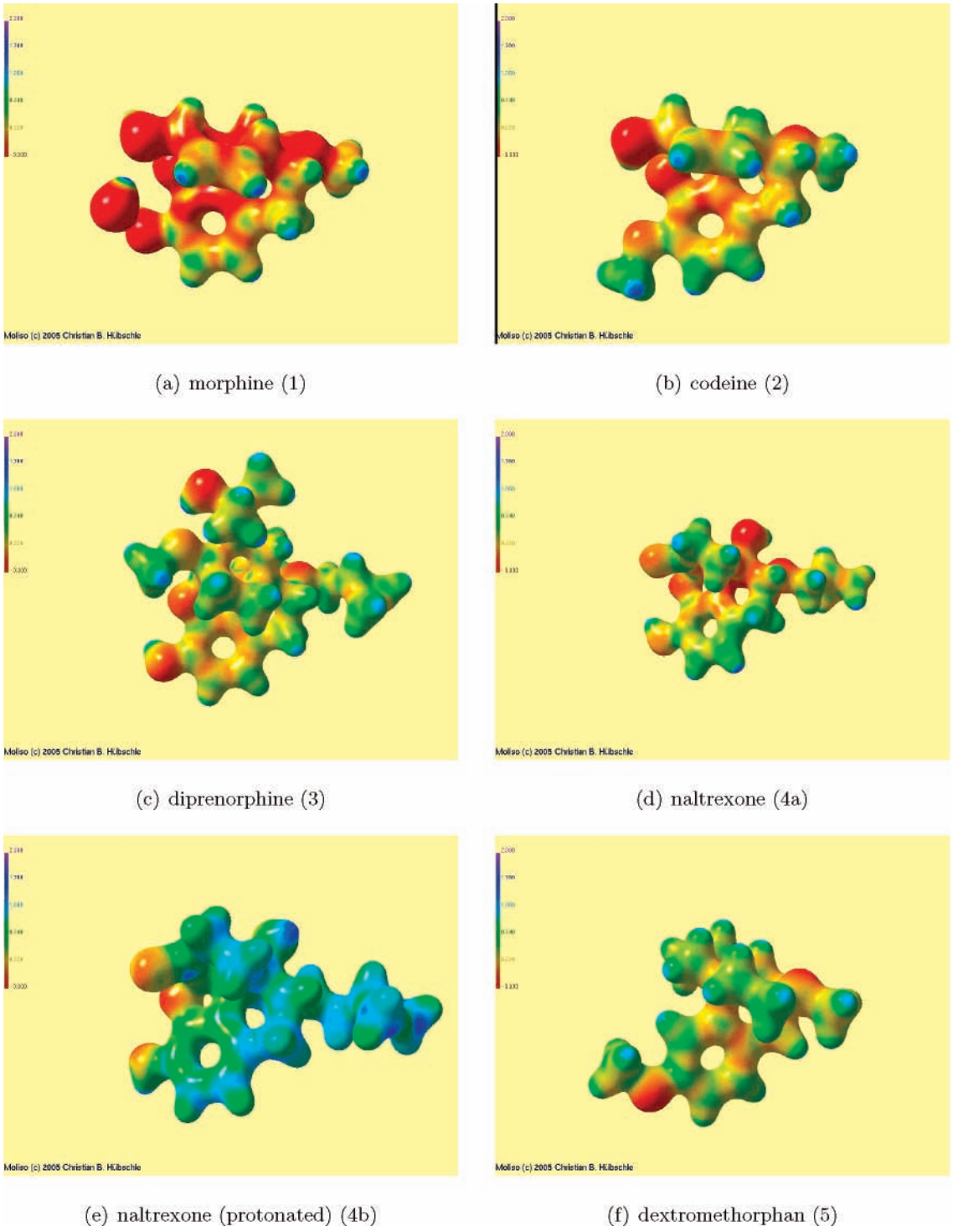

Figure 7. Three-dimensional representations of the electrostatic potential for **1**−**5** calculated from the experimental charge densities (drawing generated with MOLISO[31]). The color code is shown by the color bar.

compared to those of the free bases, the positive atomic charges of the corresponding C-atoms of **4b** show higher values, because the total charge of +1 e is not located on the formal positively charged nitrogen atom ($q = -0.62$ e) but is distributed over the neighboring carbons (see also section 5.4).

5.3. Hydrogen Bonds. The topological analysis of charge density distribution also contains topological parameters of intermolecular interactions and can give quantitative information on these interactions, in addition to the geometrical information discused in the literature, for example, by Steiner et al.[27] Geometrical and topological parameters for hydrogen bonds for the compounds are given in Table 3.

While morphine exhibits a number of strong hydrogen bonds, codeine has only two weak interactions of the type C−H···O with a low value for the electron density and a small positive value for the Laplacian at the bcp. This is found for all C−H···O bonds of the other molecules. The significance of these quantitative values should be carefully treated. Codeine represents a rare case where a hydroxyl group (O2−H21) is not involved in a hydrogen bond. This hydrogen contains interesting atomic properties. While the hydrogen atoms involved in a hydrogen bond in morphine show no significant differences between the total volume V_{tot} and V_{001} ($V_{tot} = 1.49$ Å^3 and $V_{001} = 1.47$ Å^3), the corresponding atom in codeine shows a

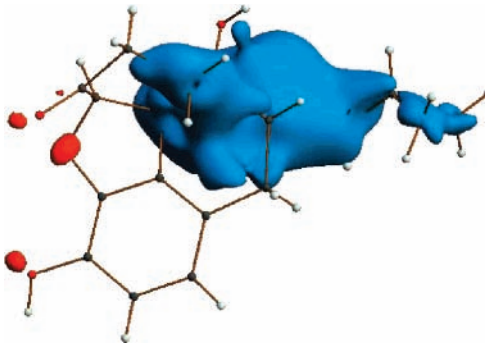

Figure 8. Isosurface representation of the difference esp between **4a** and **4b**; blue = 0.8 e Å^{-1}, red = −0.1 e Å^{-1}

difference of 27.40% (V_{tot} = 1.46 Å^3 and V_{001} = 1.06 Å^3). The atomic charge of this hydrogen atom is not affected (morphine = 0.66 e, codeine = 0.64 e). This means that the electron density of the hydrogen atom not involved in a hydrogen bond is concentrated in a smaller space.

Higher $\rho(\mathbf{r}_{bcp})$ values are found for the hydrogen bonds of medium strength. They exceed 0.1 e Å^{-3} for the N−H···O and O−H···O interactions. An exception is the hydrogen bonds of naltrexone, where the hydrogen atoms of the solvent water molecule build weaker interactions, while the corresponding oxygen atom acts as an acceptor. Table 3 also shows the hydrogen bond (HB) energies E_{HB}, calculated with the relation given by Espinosa et al.[28] (E_{HB} = 25 300 exp[−3.6(H···A)] kJ mol^{-1}, see the last column in Table 3). The 39 HBs can be divided into three groups. The first one contains the seven strong interactions with E_{HB} > 30 kJ mol^{-1}, while the second one has 30 > E_{HB} > 10 kJ mol^{-1}, and finally the last one includes the very weak interactions with E_{HB} < 10 kJ mol^{-1}.

In Figure 6, the Hirshfeld surfaces of morphine and codeine are shown. In addition, the electron density is mapped on the surface to compare especially the interaction of the nitrogen atoms. The deeply colored regions in the case of morphine confirm strong intermolecular interactions, and the contacts are significantly weaker in the case of codeine.

5.4. Electrostatic Potential. For the prediction of the reactive behavior of a chemical system, the electrostatic potential (esp) can be used. It can be derived directly from the electron density. It was calculated from the experimental data using the method of Su and Coppens[29], and it is displayed in Figure 7. The electrostatic potential is represented by a color code on the isoelectron density surface at ρ = 0.5 e Å^{-3}

An extendend negative region is accumulated around the oxygen atoms and, in most cases, around the nitrogen atoms, except in the case of the protonated naltrexone, where a positive charge concentration is observed. The atoms involved in hydrogen bonding show a stronger polarization of the electron density. As already mentioned, the esp of **4b** shows a noticeable positive potential around the nonoxygen atoms. To demonstrate the difference between the esp of **4a** and **4b**, the electrostatic potential of **4a** was subtracted from that of **4b**. For a better understanding, the positive and negative isosurfaces of the esp (blue, 0.1 e Å^{-1} and red, −0.8 e Å^{-1}) are shown in Figure 8. A small negative region is observed near the oxygen atoms, while the potentials of the aromatic ring systems cancel out each other, so that no residual potential is shown. The large positive region around the nitrogen atom and the carbon atoms in the surrounding area indicates that the formal positive charge is distributed over an extended part of the molecule.

6. Conclusion

Quantitative electronic properties were determined for codeine (**2**), diprenorphine (**3**), naltrexone (**4a** and **4b**), and dextromethorphan (**5**), including a complete topological analysis of the charge density of all the intra- and intermolecular interactions. These were compared with the topological properties of morphine (**1**) studied earlier in our group and with results obtained by theoretical calculations. Thanks to recent experimental enhancements, the series of X-ray diffraction measurements necessary for this study could be carried out in a reasonable amount of time with improved resolution and accuracy. This can, for example, be demonstrated by the two naltrexone cases (**4a**) and (**4b**). For the neutral form (**4a**), two molecules were in the asymmetric unit causing a problem of more than 100 atoms which was untouchable in the charge density field a few years before. For the protonated form (**4b**), only crystals of minor diffracting properties were available; however, data collection in front of a highly intense synchrotron beamline made it possible to obtain a reliable electron density distribution. Thus, it could be shown that synchrotron radiation is a powerful tool for charge density analysis and is even essential in certain cases. For the considered group of compounds, a high degree of reproducibility and transferability of atomic and bond topological properties could be found for those parts of the molecule having the same chemical environment. Moreover, it was possible to characterize weak interactions such as hydrogen bonds. The variance of the quantitative topological properties is in the same range as the ones found by using *ab initio* calculations with different methods and basis sets and is also in line with former studies on other oligocyclic ring systems such as strychnine.[30] On the other hand, chemical differences can be detected and visualized. The comparison of the atomic properties and the esp of the neutral and protonated form of naltrexone shows that the formal positive charge of the nitrogen atom is distributed over a large part of the molecule.

Acknowledgment. This investigation was supported by grants of the Deutsche Forschungsgemeinschaft (DFG), Grants Lu222/24-1 and 24-3, SPP1178, and the Research Training Group 788 (Hydrogen Bonding and Hydrogen Transfer).

Supporting Information Available: CCDC 643258−643262 contain supplementary crystallographic data for this paper. These data can be obtained free of charge from The Cambridge Crystallographic Data Centre. Further details of crystallographic data can be obtained from the authors upon request. A complete list of atomic and bond topological properties of compounds **1**−**5** and additional residual maps and line drawings of molecules are available free of charge via the Internet at http://pubs.acs.org.

References and Notes

(1) Flaig, R.; Koritsánszky, T.; Dittrich, B.; Wagner, A.; Luger, P. *J. Am. Chem. Soc.* **2002**, *124*, 3407−3417.

(2) Dittrich, B. Ph.D. Thesis, Free University of Berlin, 2002

(3) Pichon-Pesme, V.; Lachekar, H.; Souhassou, M.; Lecomte, C. *Acta Crystallogr., Sect. B: Struct. Sci.* **2000**, *56*, 728−737.

(4) Mebs, S.; Messerschmidt, M.; Luger, P. *Z. Kristallogr.* **2006**, *221*, 656−664.

(5) Scheins, S.; Messerschmidt, M.; Luger, P. *Acta Crystallogr., Sect. B: Struct. Sci.* **2005**, *61*, 443−448.

(6) Bader, R. F. W. *Atoms in Molecules: A Quantum Theory*, 1st ed.; The International Series of Monographs on Chemistry 22; Clarendon Press: Oxford, 1990.

(7) Holzgrabe, U.; Nachtsheim, C.; Siener, T.; Drosihn, S.; Brandt, W. *Br. J. Pharmacol.* **2006**, *147*, 153−162.

(8) Holzgrabe, U.; Nachtsheim, C.; Siener, T.; Drosihn, S.; Brandt, W. *Pharmazie* **1997**, *52*, 4−22.

(9) Drosihn, S. Ph.D. Thesis, Martin-Luther-University, Halle-Wittenberg, 1999.

(10) Pichon-Pesme, V.; Lecomte, C.; Lachekar, H. *J. Phys. Chem.* **1995**, *99*, 6242−6250.

(11) Volkov, A.; Li, X.; Koritsánszky, T.; Coppens, P. *J. Phys. Chem. A* **2004**, *108*, 4283−4300.

(12) Dittrich, B.; Hübschle, C.; Luger, P.; Spackman, M. A. *Acta Crystallogr., Sect. D: Biol. Crystallogr.* **2006**, *62*, 1325−1335.

(13) Messerschmidt, M.; Meyer, M.; Luger, P. *J. Appl. Crystallogr.* **2003**, *36*, 1452−1454.

(14) *ASTRO*, *SMART*, and *SAINT*, software programs; Burker-AXS Inc.: Madison, WI, 1997−2001.

(15) Kabsch, W. J. *J. Appl. Crystallogr.* **1993**, *26*, 795−800.

(16) Canfield, D. V.; Barrick, J.; Giessen, B. C. *Acta Crystallogr., Sect. C: Cryst. Struct. Commun.* **1987**, *43*, *977*.

(17) Swamy, G. Y. S. K. ;Ravikumar, K. ;Bhujanga Rao, A. K. S. *Acta. Crystallogr., Sect. E: Struct. Rep. Online* **2005**, *61*, 2071.

(18) Sheldrick, G. M. *SHELXL: Crystal Structure Refinement*; Universität Göttingen: Göttingen, 1997.

(19) Hansen, N. K.; Coppens, P. *Acta Crystallogr., Sect. A: Found. Crystallogr.* **1978**, *A34*, *909*−*921*.

(20) Koritsánszky, T.; Richter, T.; Macchi, P.; Volkov, A.; Gatti, C.; Howard, S.; Mallinson, P. R.; Farrugia, L.; Su, Z. W.; Hansen, N. K. *XD: A Computer Program Package for Multipole Refinement and Analysis of Electron Densities from Diffraction Data. User manual*; Freie Universität Berlin: Berlin, 2003.

(21) Allen, F. H.; Kennard, O.; Watson, D. G.; Brammer, L.; Orpen, A. G.; Taylor, R. *International Tables for Crystallography*; Kluwer Academic Publishers: Amsterdam, 1992; Vol. C.

(22) Frisch, M. J.; Trucks, G. W.; Schlegel, H. B.; Scuseria, G. E.; Robb, M. A.; Cheeseman, J. R.; Zakrzewski, V. G.; Montgomery, J. A., Jr.; Stratmann, R. E.; Burant, J. C.; Dapprich, S.; Millam, J. M.; Daniels, A. D.; Kudin, K. N.; Strain, M. C.; Farkas, O.; Tomasi, J.; Barone, V.; Cossi, M.; Cammi, R.; Mennucci, B.; Pomelli, C.; Adamo, C.; Clifford, S.; Ochterski, J.; Petersson, G. A.; Ayala, P. Y.; Cui, Q.; Morokuma, K.; Malick, D. K.; Rabuck, A. D.; Raghavachari, K.; Foresman, J. B.; Cioslowski, J.; Ortiz, J. V.; Baboul, A. G.; Stefanov, B. B.; Liu, G.; Liashenko, A.; Piskorz, P.; Komaromi, I.; Gomperts, R.; Martin, R. L.; Fox, D. J.; Keith, T.; Al-Laham, M. A.; Peng, C. Y.; Nanayakkara, A.; Challacombe, M.; Gill, P. M. W.; Johnson, B.; Chen, W.; Wong, M. W.; Andres, J. L.; Gonzalez, C.; Head-Gordon, M.; Replogle, E. S.; Pople, J. A. *GAUSSIAN98, revision A.7*; Gaussian, Inc.: Pittsburgh, PA, 1998.

(23) Cheeseman, J.; Keith, T. A.; Bader, R. F. W. *AIMPAC Program Package*; McMaster University: Hamilton, Ontario, 1992.

(24) Burnett, M. N.; Johnson, C. K., *Oak Ridge thermal ellipsoid plot program for crystal structure illustrations*; Report ORNL-6895; Oak Ridge National Laboratory: Oak Ridge, TN, 1996.

(25) Luger, P.; Messerschmidt, M.; Scheins, S.; Wagner, A. *Acta Crystallogr., Sect. A: Found. Crystallogr.* **2004**, *60*, 390−396.

(26) Volkov, A.; Gatti, C.; Abramov, Y.; Coppens, P. *Acta Crystallogr., Sect. A: Found. Crystallogr.* **2000**, *A56*, 252−258.

(27) Steiner, T. *Angew. Chem., Int. Ed.* **2002**, *41*, 48−76.

(28) Espinosa, E.; Molins, E.; Lecomte, C. *Chem. Phys. Lett.* **1998**, *285*, 170−173.

(29) Su, Z. W.; Coppens, P. *Acta Crystallogr., Sect. A: Found. Crystallogr.* **1992**, *A48*, 188−197.

(30) Messerschmidt, M.; Scheins, S.; Luger, P. *Acta. Crystallogr., Sect. B: Struct. Sci.* **2005**, *B61*, 115−121.

(31) Hübschle, C. H. *Moliso: A Program for Color Mapped Isosurfaces. User manual*; Freie Universität Berlin: Berlin, 2005.